Phase Stability, Nitrogen Vacancies, Growth Mode, and Surface Structure of ScN(001) under Sc-rich Conditions

Hamad A.H. AL-Brithen, Eugen M. Trifan, David C. Ingram, and Arthur R. Smith

Condensed Matter and Surface Science Program, Department of Physics and Astronomy, Ohio University, Athens, OH 45701

D. Gall

Department of Materials Science, Coordinated Science Laboratory, and Materials Research Laboratory, University of Illinois, 1101 West Springfield Avenue, Urbana, Illinois 61801

Abstract

Rock-salt structure scandium nitride films have been grown on magnesium oxide (001) substrates by molecular beam epitaxy using a rf plasma source for nitrogen. The case of Sc-rich growth conditions, which occurs when the scandium flux J_{Sc} exceeds the nitrogen flux J_N, is discussed. Despite the excess Sc during growth, reflection high energy electron diffraction and x-ray diffraction shows that these films have only a single orientation which is (001), and ion channeling confirms the good crystallinity. Rutherford backscattering shows that these films are off-stoichiometric, and this is found to be directly related to variations in the nitrogen, not the scandium, content by secondary ion mass spectrometry. High-resolution x-ray diffraction reciprocal lattice mapping shows that these variations in the nitrogen content are related to the existence of the N-vacancies. It is concluded that Sc-rich growth leads to the incorporation of N-vacancies into the crystal structure, the concentration of which depends on the Sc/N flux ratio. Additionally, excess scandium conditions at the surface are explored by *in-situ* scanning tunneling microscopy.

The observed wider terrace widths as compared to N-rich growth are due to an increased surface diffusion which is attributed to a Sc-rich, metallic surface structure. Combined with the large dislocation density, the enhanced diffusion results in a predominant spiral growth mode.

PACS codes: 61.50.Nw Crystal stoichiometry; 61.72.Ji Point defects; 68.37.Ef Scanning tunneling microscopy; 68.55.Ac Nucleation and growth: microscopic aspects

Keywords: scandium nitride; surface diffusion; stoichiometry; vacancies; epitaxial growth; scanning tunneling microscopy

I. INTRODUCTION

Recently, there has been much interest in scandium nitride due to its electronic properties and possibility for combination with gallium nitride.[1–10] Most reported ScN growth has been done using sputtering techniques or chemical vapor deposition methods in which the flux ratio of Sc to N during the growth is very difficult to control. An exception is Moustakas *et al.* who used ECR molecular beam epitaxy (MBE) as the growth technique.[4] More recently, Al-Brithen *et al.* reported the use of rf MBE to grow ScN; this allows the Sc:N flux ratio during growth to be carefully controlled, permitting the study of the effects of N-rich (Sc/N ratio < 1) up to Sc-rich (Sc/N ratio > 1) growth conditions.[11,12] It was found that N-rich growth conditions result in single oriented ScN (001) films with smooth surfaces. Reflection high energy electron diffraction (RHEED) during growth showed only 1×1 reconstruction. Scanning tunneling microscopy (STM) showed that the N-rich growth surface consists of plateaus and some pyramids (caused by spiral growth around dislocations) with a single atomic step height between terraces equal to half the lattice constant, 2.25Å. It was also shown by Rutherford Backscattering that these films are stoichiometric (N/Sc = 1 to within the RBS accuracy $\sim 2\%$).

The formation of non-stoichiometric transition metal nitrides has been a topic of great interest for many years. Titanium nitride, for example, is remarkable in that it can sustain a substantial range of composition variation while remaining single phase (rocksalt structure), thus implicating the existence of both N and Ti vacancies.[13] In the case of ScN (also rocksalt structure) on the other hand, Porte reported the coexistence of two separate phases in under-stoichiometric sputtered ScN films which were prepared with lower N overpressures - ScN and Sc metal - as opposed to ScN_x with x less than 1.[10] It was argued that the absence of N-vacancies (not more than 0.5%) was due to their being energetically unfavorable. In our recent work, however, we have found a very different result - namely that growth of ScN by rf MBE results in quite high N-vacancy concentrations (up to 20%) if the Sc flux exceeds the N flux.[12] Moreover, we have shown that such films are also smooth and highly

crystalline; nevertheless, the N-vacancies do affect the electrical and optical properties. In this paper, we concentrate on the issue of off-stoichiometric ScN, presenting new data which confirms the stability of the rocksalt phase, the (001) orientation, and the existence of substantial concentrations of nitrogen vacancies. In addition, we also discuss the issue of surface structure and surface adatom diffusion and how these affect the smooth growth morphology of these off-stoichiometric ScN films.

II. EXPERIMENTAL PROCEDURE

ScN layers are grown by MBE on MgO(001), using a radio frequency (RF) plasma source for nitrogen and an effusion cell for scandium. Details of the MBE growth setup and substrate cleaning procedure are published elsewhere.[11,12] ScN growth takes place with the substrate set at $\sim$ 800 °C and the base pressure of nitrogen set at 9×10^{-6} torr with the N_2 flow rate of about 1.1 sccm.

The growth starts when the scandium shutter is opened. Scandium rich growth conditions occur when the Sc flux, J_{Sc}, exceeds the N flux, J_N. The average scandium flux J_{Sc} is determined by measuring the final film thickness using a thickness profilometer; from this, and by knowing the growth time and Sc atomic density in ScN, the Sc flux J_{Sc} is calculated. The effective N flux is determined to be $J_N \sim 3.6{\times}10^{14}$ cm^{-2} s^{-1} in our system for the stated conditions.[12] The flux ratio (J_{Sc}/J_N) can be adjusted by changing the scandium effusion cell temperature.

The growth is monitored in real time using RHEED. Following growth, samples can be transferred under vacuum to the scanning tunneling microscope for surface analysis. After taking the sample out of the chamber, it is analyzed using x-ray diffraction (XRD) with a Rigaku $\theta - 2\theta$ diffractometer having Cu $K\alpha$ radiation. Small pieces are also provided for analysis by Rutherford backscattering (RBS), ion channeling, XRD reciprocal lattice mapping, and secondary ion mass spectrometry (SIMS) [Charles Evans and Associates, Sunnyvale, CA].

III. RESULTS AND DISCUSSION

A. Crystallinity and Orientation

In Fig. 1 is shown the XRD 2θ scan for a ScN film grown on MgO(001) under Sc-rich conditions ($J_{Sc}/J_N = 1.17$) displayed on log scale. The MgO 002 substrate peak appears at 42.94°, and the ScN 002 peak appears at 39.99°. The MgO 004 and ScN 004 peaks are also seen at 93.99° and 86.14°, respectively. As can be seen, no other peaks are observed. Therefore this sample, although grown under Sc-rich conditions, is highly crystalline with (001) orientation. From the positions of the peaks, the perpendicular lattice parameter for this sample is calculated to be $a_{ScN} = 4.509$ Å, slightly above the bulk relaxed value of stoichiometric ScN = 4.501 Å,[6] indicating mild compressive strain due to differential thermal contraction during cooling from growth temperature, 800°C, to room temperature. While this film has near ideal crystallinity, it will be shown below that it contains a large nitrogen deficiency.

Further evidence for the crystalline nature of these films is obtained from RBS, which has been performed for samples using a helium ion beam of incident energy of 2.189 MeV and a backscattering angle of 168°. Shown in Fig. 2(a) is a plot of the backscattering yield as a function of energy for a ScN film grown under slightly Sc-rich conditions ($J_{Sc}/J_N \sim 1.03$). Two results are shown - one for the sample [001]-direction randomly oriented with respect to the incident beam and the other for the sample [001]-direction aligned parallel to the incident beam. The scandium edge begins at $\sim$ 1.55 MeV (film surface) and ends at about 1.25 MeV (substrate-film interface) while the N edge begins at $\sim$ 0.7 MeV (film surface) and ends at $\sim$ 0.4 MeV (substrate-film interface). The substrate edges for magnesium and oxygen begin at $\sim$ 0.83 and 0.52 MeV, respectively.

It is clearly seen that the aligned spectrum has dramatically reduced backscattering yield compared to the non-aligned spectrum, showing that the channeling is extremely high along the [001] direction. The computed χ_{min} for Sc, which is the ratio of the counts of the aligned

spectrum to the counts of the non-aligned spectrum (at channel 210), is just 2.4%. Fig. 2(b) shows the 2-D ion channeling rocking scan. The Z-axis represents the total charge of the incident beam needed to produce a constant backscattered beam intensity while the X- and Y-axes represent the angular position of ScN[001] direction with respect to the incident beam. Therefore, orientations with higher channeling appear as higher points in the plot. The plot shows clearly the symmetry of the rocksalt lattice, with a strong central peak corresponding to channeling along [001] and clear ridges corresponding to 4-fold symmetry directions. These data further support the conclusion that the sample is a highly oriented, epitaxial, crystalline film.

B. Nitrogen Vacancies

RBS data is also used to determine the stoichiometry of the ScN films by fitting the RBS spectra using the RUMP simulation code.[14] The result gives the average Sc/N bulk composition ratio. This has been done for samples grown with various flux ratios. It was found that for a flux ratio J_{Sc}/J_N equal to 0.26 ± 0.03, RBS gives a Sc/N composition ratio equal to 1.00 ± 0.02. For J_{Sc}/J_N= 1.03 ± 0.03, RBS gives a composition ratio equal to 1.00 ± 0.02. Finally, for J_{Sc}/J_N= 1.17 ± 0.03, RBS gives a composition ratio equal to 1.20 ± 0.02. This shows that N-rich conditions result in stoichiometric films (Sc/N = 1) while Sc-rich conditions result in non-stoichiometric films, and it shows that the bulk Sc/N composition ratio agrees well with the Sc/N flux ratio (within a few %) in the case of Sc-rich conditions.[12]

To determine variations in the composition ratio as a function of growth time, SIMS has been performed. In Fig. 3 is shown the SIMS depth profile for the non-stoichiometric ScN film having an average bulk composition ratio Sc/N of 1.20 ± 0.02, as determined from RBS. The total film thickness was about 6000 Å. Although there are no ScN standards to determine absolute concentrations of Sc and N from SIMS data, changes in the signals indicate variations in the bulk concentrations. As is seen, both Sc and N signals are nearly

constant until $\sim$ 2800 Å, indicating a fairly constant Sc/N bulk ratio. At 2800 Å, the Sc/N flux ratio was increased. What is seen is not an increase in the Sc signal but rather a decrease of about 4% in the N signal. Then, at 4900 Å, the Sc/N flux ratio was again increased, and again the N signal is observed to decrease, by about 2%. Throughout the entire growth, the scandium signal is nearly constant, independent of the Sc/N flux ratio, while the N signal changes several times.

Assuming that the sputtering rate is dependent on (e.g. inversely proportional to) the Sc density, it is understandable that the Sc signal should remain constant, independent of potential variations in the Sc density. In this case, it would be possible to obtain false variations in the N signal. However, since the growth rate of ScN goes linearly proportional to the Sc flux (for N- or Sc-rich conditions), and since we do not observe the formation of Sc precipitates, it is more likely that the Sc density is in fact constant throughout the film, as the SIMS profile suggests. Moreover, if the changes in N signal were due only to variations in the sputtering rate, then corresponding changes should also have been observed at the same depths in the simultaneously measured C and O signals (not shown); such changes were not observed. Therefore, we conclude that changes in the N signal correspond directly to changes in the N density and thus that the N density varies with depth according to the Sc/N flux ratio in Sc-rich conditions, and attribute these changes in N density to variations in the number of N vacancies.

In order to confirm that the composition variations are actually due to N-vacancies and not for example related to antisite substitutions, we performed high-resolution x-ray diffraction reciprocal lattice mapping (HRRLM) on asymmetric 224 reflections in order to determine the relaxed lattice constant $a_\circ$ as a function of Sc/N flux ratio, following the procedure described elsewhere.[15] Measured lattice constants perpendicular and parallel to the layer surface provide, together with the Poisson ratio $\nu_{ScN} = 0.20$,[16] values for $a_\circ = 4.503 \pm 0.002$ Å, which were found to be independent of the Sc/N flux ratio. Thus, there is no detectable change in $a_\circ$ over the entire composition range $1.00 \leq \mathrm{Sc/N} \leq 1.17$. *Ab initio*

density functional calculations employing the generalized gradient approximation, periodic boundary conditions, and 16-atom supercells show that ScN_x with x = 0.88 has an $a_\circ$ which is almost identical (only 0.1 % smaller) to the stoichiometric ScN lattice constant if the N-deficiency is accounted for by N-vacancies. However, Sc on N antisite substitutions or Sc-interstitials result, for layers with x = 0.88, in a considerable increase of $a_\circ$ by 1.4% or 5.1%, respectively. Thus, the experimentally observed absence of a change in $a_\circ$ with Sc/N ratio is, within uncertainty, consistent with the presence of N-vacancies. In contrast, if the N deficiency in the layers grown with Sc/N > 1 would be due to antisite substitutions or Sc-interstitials, the change in $a_\circ$ would be clearly observable by our HRRLM experiments. Therefore, the reciprocal lattice mapping results show, in agreement with our SIMS data, that the deviations from stoiciometry for Sc/N > 1 are due to N-vacancies.

As discussed in the previous section, XRD and RBS channeling both show ideal crystallinity. Therefore, for rf MBE growth in Sc-rich conditions, the rocksalt crystal structure is apparently able to accommodate relatively high N-vacancy concentrations (up to 20%).[11,12] Thus, Porte's earlier work, which reported that sub-stoichiometric ScN films contain no N-vacancies but instead separated phases of ScN and Sc metal, seems not to be a general conclusion but rather a result specific to a certain growth technique (i.e. reactive sputtering followed by annealing).[10]

Recently, Stampfl *et al.*, using density functional theory and a screened-exchange local density approximation (sX-LDA) method as well as the LDA, calculated the (neutral) bulk N-vacancy formation energy.[17] While this energy is quite high in the case of N-rich conditions (4.32 eV), it is much lower and in fact just slightly negative in the case of Sc-rich conditions (-0.42 eV). Therefore, while N-vacancies are not easily formed under N-rich growth conditions, they can easily form under Sc-rich growth conditions. The same group also calculated the (neutral) bulk Sc-vacancy formation energies and found them to be very high for both Sc-rich and N-rich conditions, indicating that Sc-vacancies are energetically unfavorable which agrees with our experimental observations of constant Sc density.

C. Growth Mode and Surface Diffusion Barriers

Shown in Fig. 4 is a STM image of the surface of the ScN(001) film grown on MgO(001) at the flux ratio $J_{Sc}/J_N = 1.03$.[12] The surface consists of big rounded spiral mounds, and smooth terraces are also observed, confirming that the growth is epitaxial. The step height between terraces is equal to $a_{ScN}/2 = 2.25$ Å, which is one atomic layer of ScN. The spiral mounds also contain pits which are seen near the mound centers; some other pits which are not at the mound centers are also observed, and these are correlated with the termination (or emanation) of one or more steps. It is therefore concluded that the pits at the mound centers or elsewhere are each correlated with the presence of a dislocation. Those dislocations near the mound centers evidently have a screw component of the Burgers vector while the others may have only edge components. By assuming one dislocation per pit, the total dislocation density is estimated to be $\sim 1\times 10^{10}\ cm^{-2}$. The slip line seen at lower left corner of Fig. 4 is attributed to thermal stress as the sample temperature was changed.

Spiral growth has also been observed under metal-rich conditions in the case of GaN(0001), as reported by several groups.[18–23] For example, Tarsa *et al.* showed that the surface of GaN(0001) grown under Ga-rich conditions consists of spiraling hillocks as seen using atomic force microscopy.[19,21] Also, Smith *et al.*, using *in-situ* STM, observed growth spirals on the GaN(0001) surface for Ga-rich growth conditions.[22] On the other hand, the GaN(0001) surface becomes rough under N-rich conditions which has been attributed to a kinetic accumulation of excess N on the surface combined with the fact that neither experiment nor theory finds an energetically stable N-terminated surface for GaN (0001) or $(000\bar{1})$, as noted by Feenstra *et al.*[23,24] The behavior is related to the strong Ga−N bonds formed at the surface under N-rich conditions which substantially increase the diffusion barriers for Ga adatoms; Ga−Ga bonds which predominate under Ga-rich conditions are weaker, and this leads to lower diffusion barriers. Zywietz *et al.* determined, based on density functional theory, the difference in diffusion barriers for Ga adatoms in Ga-rich conditions compared to N-rich conditions for both GaN (0001) and $(000\bar{1})$ surfaces, finding values of 1.4 eV and

0.8 eV, respectively.[24]

The transition to a rounded spiral growth mode for these two systems (ScN and GaN) under metal-rich conditions suggests a common origin despite their very different crystal structures (rocksalt vs. wurzite). In the case of ScN, we recently estimated using STM measurements, the difference in surface diffusion barriers for Sc-rich conditions versus N-rich conditions to be about 0.26 eV, Sc-rich conditions having the lower barrier.[12] We note that this is a much smaller difference compared to the case of GaN, consistent with the fact that atomically smooth and well-ordered surfaces of ScN(001) are also observed for N-rich conditions.[11] Since we do not observe a roughening of the ScN(001) surface under N-rich conditions, this suggests that N adatoms do not accumulate on the surface; rather, the excess N leaves the surface.

If a Sc-rich surface structure exists for ScN(001), the decrease in the surface diffusion barrier in going to Sc-rich conditions may also be a consequence of weaker metallic Sc−Sc bonding as compared with Sc−N bonding at the surface. From the CRC table of diatomic bond strengths,[28] the metallic Sc−Sc bond strength is 1.69 ± 0.22 eV which is weaker than the Sc−N bond strength which is 4.87 ± 0.87 eV. These numbers are comparable to the case of GaN. From the CRC table, the bond strength of Ga-Ga is 1.43 ± 0.22 eV, slightly weaker than Sc-Sc. This is interesting since the melting point of Ga (303 K) is so much lower than that of Sc (1812 K); however, the dissociation energies are similar (e.g. to reach a common vapor pressure of 2×10^{-4} torr, we need $T_{Ga} = 1223$ K and $T_{Sc} = 1423$ K). Finally, while the Sc−N bond has more ionic character than the Ga−N bond (due to a larger electronegativity difference), the Sc−N bond has about the same strength as the Ga−N bond. For example, the melting point of ScN was reported to be 2873 ± 50 K,[25] whereas the melting point of GaN was theoretically estimated to be 2791 K.[26] Thus, the common origin of the growth behavior between ScN and GaN may be related to the similarity in their bonding energies.

D. Scandium Rich Surface Structure

The drop in surface diffusion barrier upon crossing into Sc-rich conditions suggests a corresponding qualitative change in the surface structure. In the case of GaN(0001), it was found that the surface structure which forms under Ga-rich conditions has approximately two additional monolayers of Ga on top of the Ga-terminated bilayer whereas these monolayers disappear under N-rich conditions.[22,23,29] In the case of ScN, Stampfl *et al.* have recently calculated various surface structural models, including ideal-relaxed (bulk terminated), Sc-terminated, 2Sc-terminated and N-vacancy models.[17] They found that the ideal-relaxed 1×1 model is energetically most favorable over a wide range of nitrogen chemical potential, including the N-rich end of the range. This result was also obtained via first-principles calculations by Takeuchi.[30]

For Sc-rich conditions, Stampfl *et al.* calculated that a 2×1 N-vacancy model would be energetically most favorable within a small range of chemical potential on the Sc-rich side.[17] Their 2×1 N-vacancy model consists of rows of surface N-vacancies running along [110]. In addition, their 1×1 Sc-terminated model was also found to be lower in energy than the ideal surface under Sc-rich conditions but a little higher in energy than the 2×1. Both the 2×1, in which half the surface N-sites are vacancies, and the 1×1 Sc-terminated models, in which all N-sites are vacancies, have substantial metallic bonding character.[17] This is consistent with our recent tunneling spectroscopy experiments on ScN(001) grown under Sc-rich conditions where we find metallic surface states.[27]

Displayed in Fig. 5 are STM images at higher resolution of a ScN(001) surface acquired following growth under Sc-rich conditions. Dashed lines in each image enclose the identical surface region for comparison. At a sample bias of +2.0 V, as shown in Fig. 5(a), smooth terraces are observed with meandering steps; the minimum step height between terraces is a single atomic layer or half the lattice constant of ScN = 2.25 Å. Aside from some tiny dark pocks, very little structure is seen on the terraces, consistent with a metallic surface. More detail can be seen at a lower sample bias of +1.0 V, as shown in Fig. 5(b). Here one

observes a random-looking distribution of nanometer-sized protrusions. These protrusions are numerous, appearing to occupy a large fraction of the surface area. As a result, the step edges are somewhat less distinct but still visible.

While no well-ordered surface reconstruction is evident, the structure of the surface grown under Sc-rich conditions is clearly very different compared to that grown under N-rich conditions. In addition, the fact that the surface is very smooth with well defined step edges implies that the growth follows the step-flow mode; therefore, the protrusions seen in the STM images of Fig. 5(b) are not nucleation centers (i.e. new ScN islands) but rather are related to the intrinsic structure of the terrace. And since the surface exhibits metallic conductivity, we conclude that the top layer contains an excess of Sc metal. It is thus likely that the tiny protrusions correspond to scandium-rich clusters which are similar in structure to the Sc-terminated reconstruction - namely that they are deficient in N atoms. The clustering could be related to the instability of the Sc-terminated reconstruction and could provide a mechanism for lowering the surface energy. The regions between the protrusions most likely correspond to the more bulk-like second layer.

Shown in Fig. 6 are schematic side-view models of the ScN(001) surface in (a) N-rich conditions and (b) Sc-rich conditions. For N-rich conditions, the surface is stoichiometric and the step edge is distinct. For Sc-rich conditions, the excess Sc atoms in the top layer make the step edge appear less distinct, consistent with the STM image of Fig. 5(b). Such a Sc-terminated surface would have metallic character, could be established during Sc-rich growth, and is qualitatively consistent with the Sc-rich surface models proposed by Stampfl *et al.* Note that the surface stoichiometry is independent of the bulk stoichiometry. For example, the top layer could contain 100% N vacancies while the bulk contained only a few % N vacancies (depending on the flux ratio).

Further evidence that the Sc-rich surface top-layer contains mainly Sc has recently been obtained. The RHEED patterns for Sc-rich growth always show clear first-order streaks, as we have previously reported.[11,12] However, some very weak half-order streaks are occasionally observed along [110], as shown in the RHEED pattern in Fig. 7(a). These are more clearly

evident in the averaged line profile shown in Fig. 7(b). Weak half-order streaks are consistent with a small amount of ordering of surface atoms into the 2×1 N-vacancy reconstruction predicted by Stampfl *et al.*[17]. In this case the top layer would contain some nitrogen atoms. However, we have so far not observed any well-ordered 2×1 regions by STM.

To explore the 2×1 seen in RHEED further, another experiment was performed. The ScN growth was initiated on MgO(001) under Sc-rich conditions, and the RHEED pattern showed a weak 2× from the very beginning. Later during the growth, the Sc/N flux ratio was reduced. Surprisingly, the 2× pattern remained. Even for very low Sc/N flux ratio, the weak half-order streaks did not disappear. This suggests that surface N-vacancy ordering may lead to bulk ordering. Bulk ordering of N-vacancies is prevalent in manganese nitride, as we have observed in our recent studies of that material.[31] However, the 2× streaks seen in Fig. 7 are not always observed, and we have seen no other evidence for bulk N-vacancy ordering in ScN. Thus, the basic rock-salt structure is very stable, even with the presence of significant quantities of N-vacancies.

IV. SUMMARY

We have studied the epitaxial growth of ScN on MgO(001) substrates under Sc-rich conditions using rf MBE. XRD and RBS confirm that the rocksalt phase is maintained and that the films have good crystallinity with (001) orientation. SIMS shows that only the N density changes when the flux ratio J_{Sc}/J_N is changed; the Sc density remains constant which indicates that the film has a N vacancy concentration which depends on the Sc/N flux ratio under Sc-rich conditions. The relaxed lattice parameter remains constant with changing Sc/N flux ratio, confirming that the N-deficiency in layers grown under Sc-rich conditions is due to N-vacancies. Large-scale STM images show that Sc-rich growth conditions result in the spiral growth mode with large mounds and smooth terraces. The increased terrace widths compared to N-rich growth conditions indicate increased surface adatom diffusion. Detailed STM images of the surface strongly suggest a metal-rich, metallic surface layer.

The spiraling growth mode can therefore be attributed to enhanced surface diffusion due to weaker Sc-Sc bonding. The RHEED pattern for Sc-rich conditions occasionally shows weak half-order streaks along [110], indicating a small degree of surface ordering which may be related to the 2×1 N-vacancy reconstruction predicted by Stampfl *et al.* Note the resulting bulk stoichiometry will be directly related to the flux ratio, not the surface stoichiometry. Lastly, while Sc-rich conditions result in lower diffusion barriers, the excess Sc results in N-vacancies which have detrimental effects on the bulk optical properties.[12]

V. ACKNOWLEDGEMENTS

This work has been supported by the Office of Naval Research and the National Science Foundation under grant No. 9983816. The authors also wish to thank M. Kordesch, S. Ulloa, N. Takeuchi Tan, C. Stampfl, and R. M. Feenstra for useful discussions and F. Perjeru for help in preparing substrates. Funding by the W. M. Keck Foundation is gratefully acknowledged. We also thank J. D'Arcy-Gall for performing HRRLM measurements and appreciate the use of the facilities at the Center for Microanalysis of Materials at the University of Illinois.

REFERENCES

[1] M. Little and M. E. Kordesch, Appl. Phys. Lett. **78**, 2891 (2001).

[2] F. Perjeru, X. Bai, M. I. Ortiz-Libreros, R. Higgins, M. E. Kordesch, Appl. Surf. Sci., **175-176**, 491 (2001); F. Perjeru, X. Bai, and M. E. Kordesch, Appl. Phys. Lett. **80**, 995 (2002).

[3] J. P. Dismukes, W. M. Yim, and V. S. Ban, J. Cryst. Growth **13/14**, 365 (1972).

[4] T. D. Moustakas, R. J. Molnar, and J. P. Dismukes, Proc.-Electrochem. Soc. **96-11**, 197 (1996).

[5] D. Gall, I. Petrov, L. D. Madsen, J. E. Sundgren, and J. E. Greene, Vac. Sci. Technol. A **16**, 2411 (1998).

[6] D. Gall, I. Petrov, N. Hellgren, L. Hultman, J. E. Sundgren, and J. E. Greene, J. Appl. Phys. **84**, 6034 (1998).

[7] X. Bai, and M. E. Kordesch, Appl. Surf. Sci., **175-176**, 499 (2001).

[8] C. Stampfl, W. Mannstadt, R. Asahi, and A. J. Freeman, Phys. Rev. B **6315(15)**, 5106 (2001).

[9] W. R. L. Lambrecht, Phys. Rev. B **62**, 13538 (2000).

[10] L. Porte, J. Phys. C: Solid State Phys. 18 (1985) 6701-6709

[11] H. A. AL-Brithen, and A. R. Smith, Appl. Phys. Lett., **77**(16), 2485 (2000).

[12] A. R. Smith, H. A. H. Al-Brithen, D. C. Ingram, and D. Gall, J. Appl. Phys. **90(4)**, 1809 (2001).

[13] J.-E. Sundgren, B.O. Johansson, A. Rockett, S. A. Barnett, and J. E. Greene, *Physics and Chemistry of Protective Coatings*, edited by J.E. Greene, W.D. Sproul, and J.A. Thornton, American Institute of Physics Series **149** (AIP, New York, 1986), p. 149.

[14] L. R. Doolittle, Nucl. Inst. Meth. **B9**, 334 (1985).

[15] C.-S. Shin, D. Gall, Y,-W. Kim, P. Desjardins, I. Petrov, J. E. Greene, M. Oden, and L. Hultman, J. Appl. Phys. **90**, 2879 (2001).

[16] D. Gall, I. Petrov, P. Desjardins, and J. E. Greene, J. Appl. Phys. 86, 5524 (1999).

[17] C. Stampfl, R. Asahi, and A. J. Freeman, submitted to Phys. Rev. B.

[18] A. R. Smith, R. M. Feenstra, D. W. Greve, J. Neugebauer, and J. E. Northrup, Appl. Phys. A **66**, S947 (1998).

[19] E. J. Tarsa, B. Heying, X. H. Wu, P. Fini, S. P. DenBaars, and J. S. Speck, J. Appl. Phys. **82(11)**, 5472 (1997).

[20] R. A. Held, D. E. Crawford, A. M. Johnston, A. M. Dabiran, and P. I. Cohen, J. Electron. Mater. **26**, 272 (1997); R. A. Held, G. Nowak, B. E. Ishuang, S. M. Seutter, A. Parkhomovsky, A. M. Dabiran, P. I. Cohen, I. Grzegory, and S. Porowski, J. Appl. Phys. **85**, 7697 (1999).

[21] B. Heying, E. J. Tarsa, C. R. Elsass, P. DenBaars, and J. S. Speck, J. Appl. Phys. **85**, 6470 (1999).

[22] A. R. Smith, R. M. Feenstra, D. W. Greve, M. S. Shin, M. Skowronski, J. Neugebauer, and J. E. Northrup, J. Vac. Sci. Technol. **B 16(4)**, 2242 (1998).

[23] R. M. Feenstra, H. Chen, V. Ramachandran, C. D. Lee, A. R. Smith, J. E. Northrup, T. Zywietz, J. Neugebauer, and D. W. Greve, Surf. Rev. & Lett. **7 (5-6)**, 601 (2000).

[24] Tosja Zywietz, Jorg Neugebauer, and Matthias Scheffler, Appl. Phys. Lett. **73(4)**, 487 (1998).

[25] C. T. Horovitz, ed. *et al.*, *Scandium : its occurrence, ...*, London; New York: Academic Press, 165 (1975).

[26] J. A. Van Vechten, Phys. Rev. B **7**, 1479 (1973).

[27] H. Al-Brithen *et al.*, to be published.

[28] Handbook of Chemistry and Physics, CRC Press, 64th Edition, F176-181 (1983-4).

[29] J. E. Northrup, J. Neugebauer, R. M. Feenstra, and A. R. Smith, Phys. Rev. B **61**, 9932 (2000).

[30] N. Takeuchi Tan and S. Ulloa , submitted to Phys. Rev. B.

[31] H. Yang, H. Al-Brithen, A. R. Smith, J. A. Borchers, R. L. Cappelletti, and M. D. Vaudin, Appl. Phys. Lett. **77**, 3860 (2001).

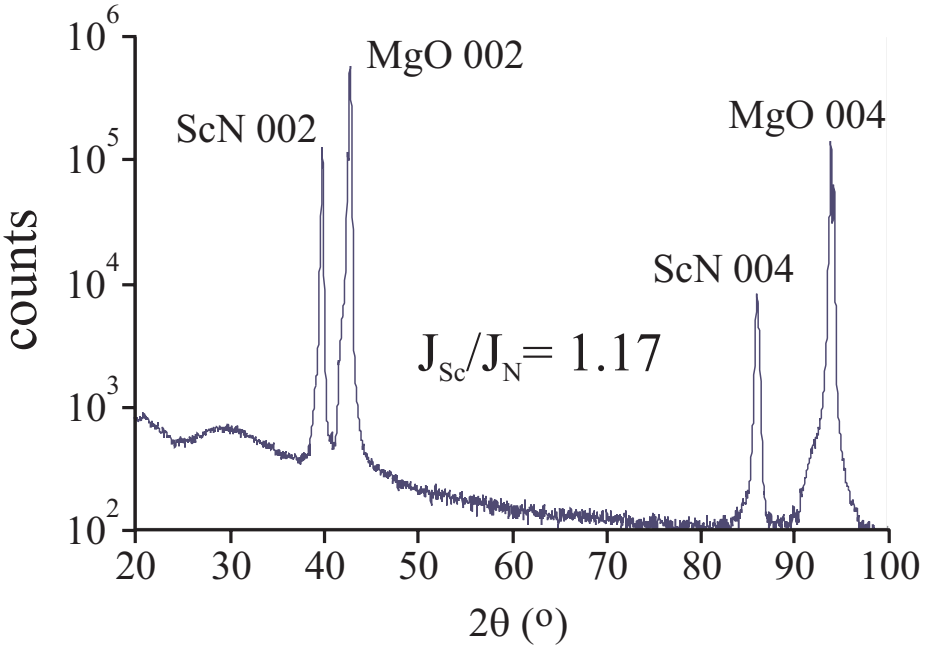

FIG. 1. XRD 2θ scan for ScN film grown under scandium rich conditions.

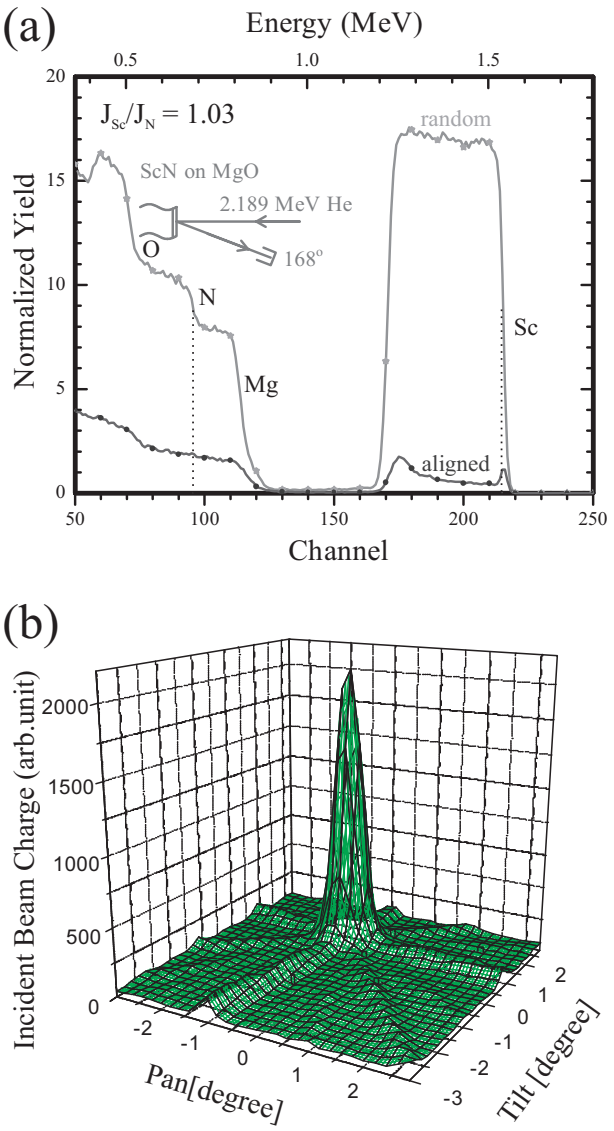

FIG. 2. (a) RBS channeling for ScN(001) film randomly aligned and well aligned with the incident beam. The film was grown under slightly Sc-rich conditions. (b) the RBS rocking scan for the same film.

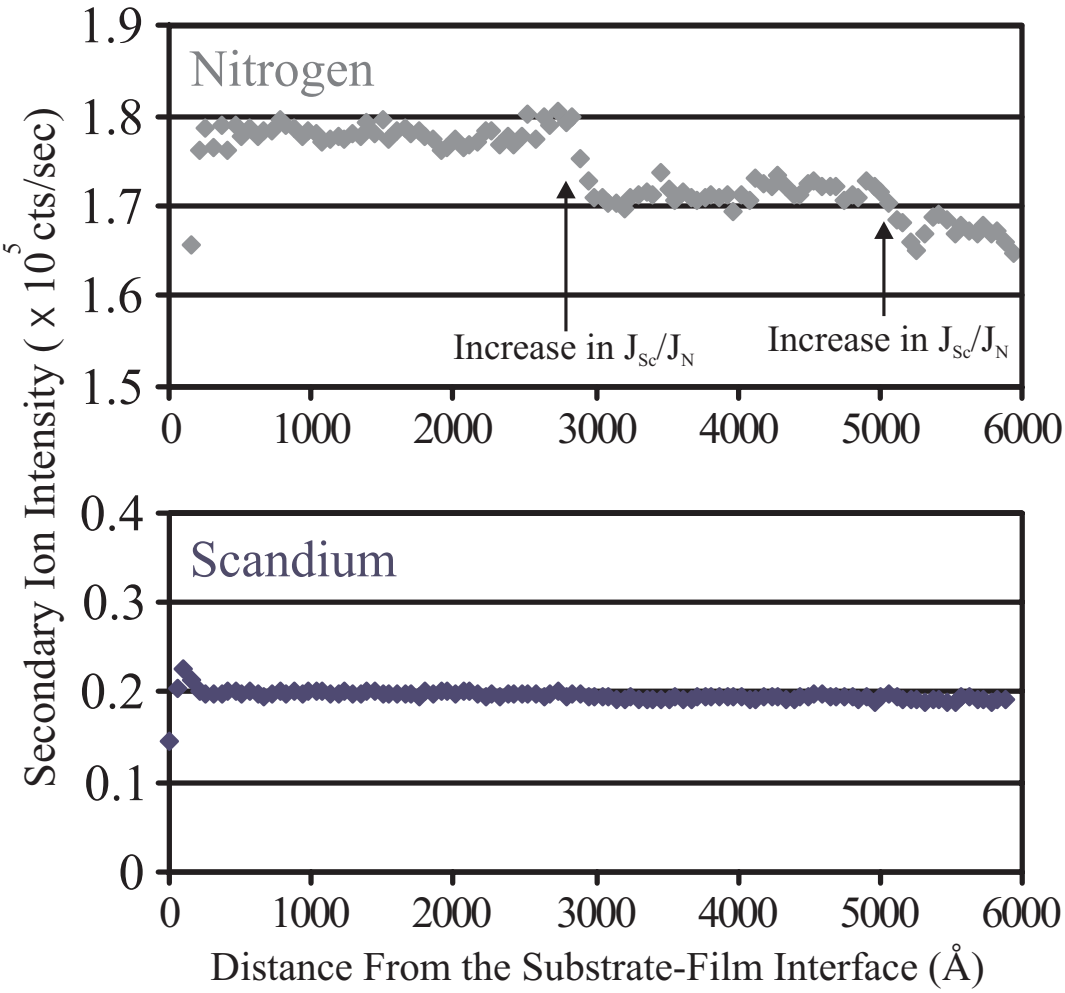

FIG. 3. SIMS profile as a function of distance from the substrate-film interface for a ScN(001) film grown under Sc-rich conditions and with changing flux ratio J_{Sc}/J_N (*measurements by Charles Evans and Associates*).

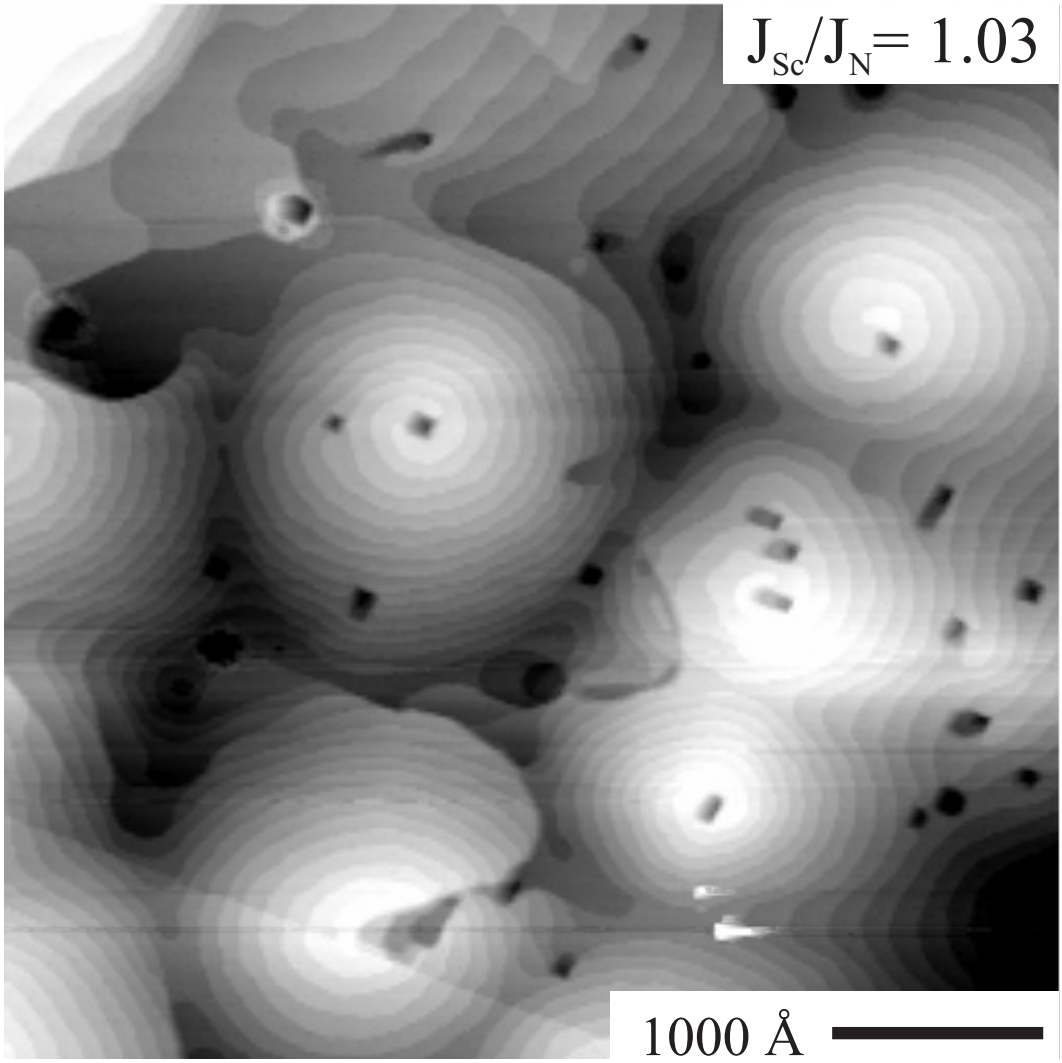

FIG. 4. STM image of ScN(001) surface grown under scandium rich conditions. Sample bias = +2.0 V; tunneling current = 0.2 nA.

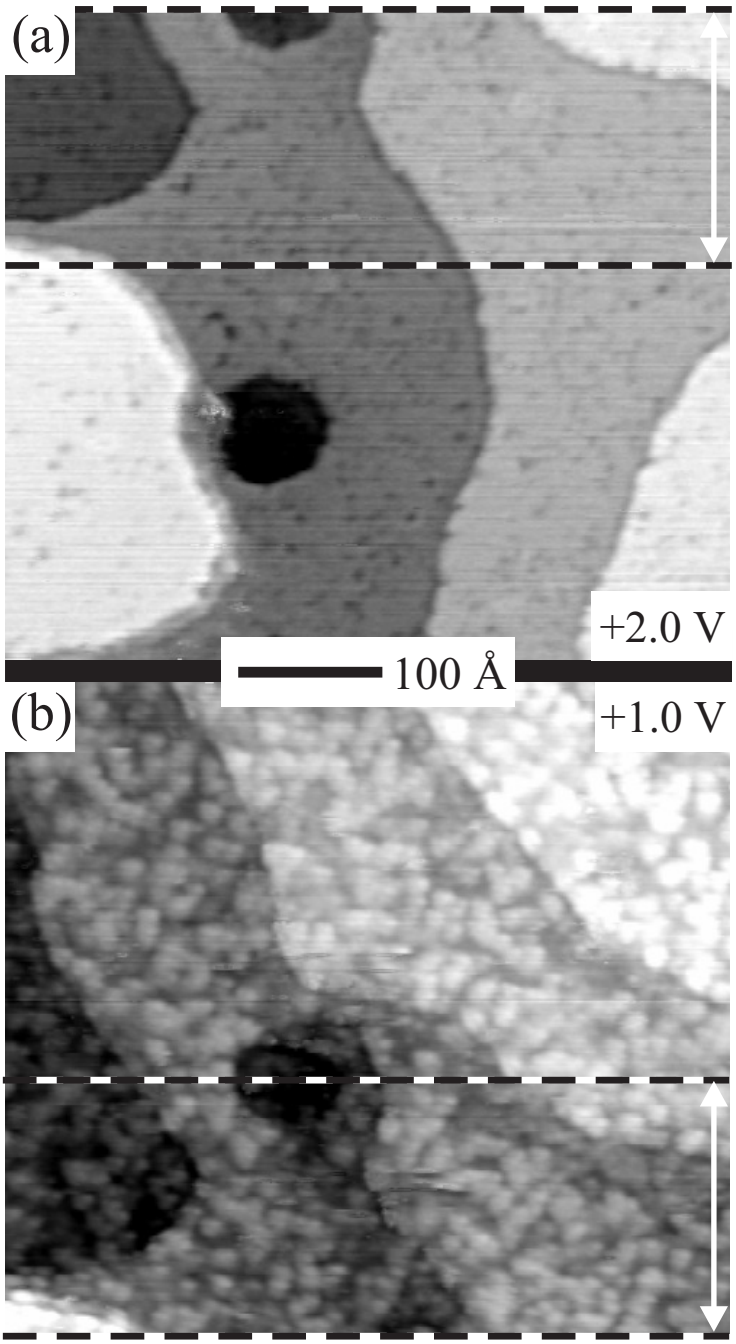

FIG. 5. STM images of ScN(001) surface grown under scandium-rich conditions. a) sample voltage = +2.0 V, tunneling current = 0.2 nA; b) sample voltage = +1.0 V, tunneling current = 0.2 nA. The areas between the dashed lines in the two images correspond to the same surface region.

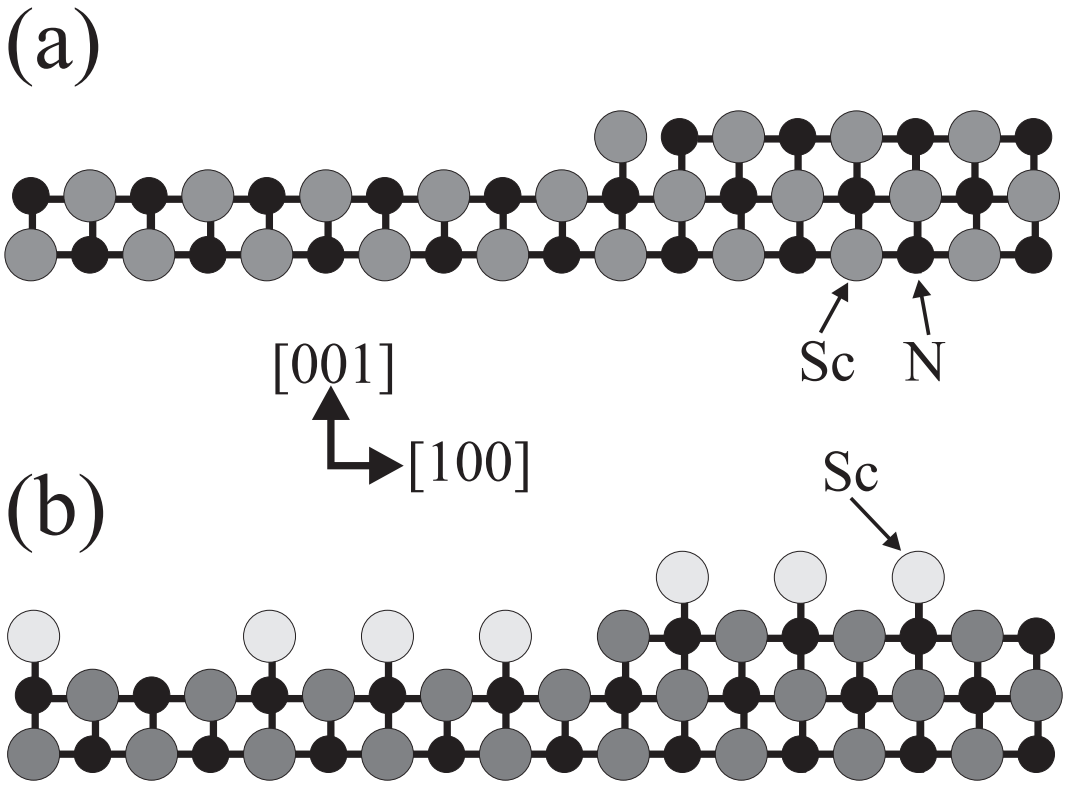

FIG. 6. Schematic side-view atomic models of (a) ScN(001) under N-rich conditions having bulk-like top layer and (b) ScN(001) under Sc-rich conditions having Sc-clusters as the top layer.

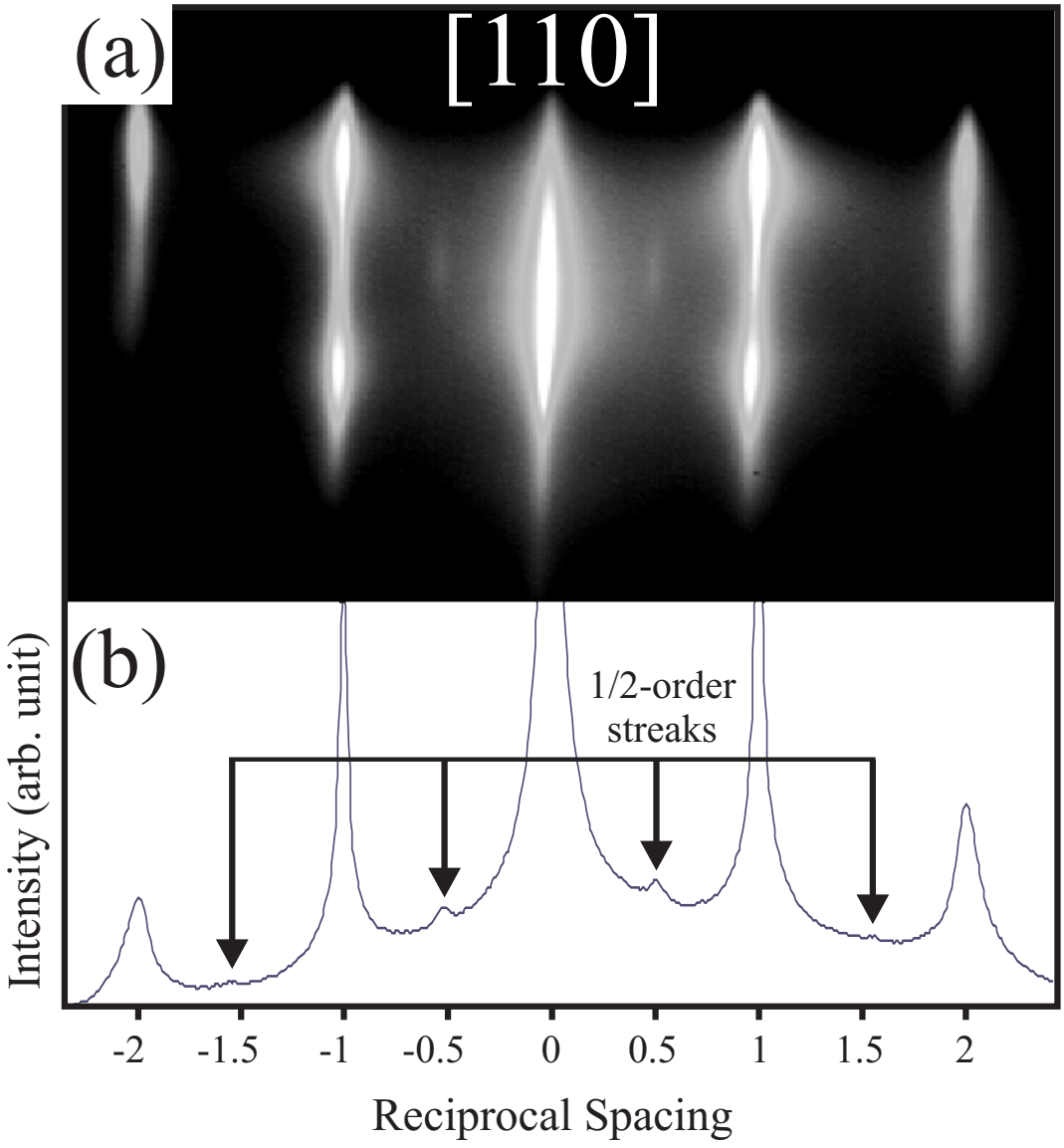

FIG. 7. (a) RHEED pattern along [110] for ScN(001) under Sc-rich conditions, and (b) the averaged horizontal line profile showing the existence of 2×.